Syntheses, Crystal Structures, and Magnetic Properties of One-Dimensional Oxalato-Bridged Co(II), Ni(II), and Cu(II) Complexes with *n*-Aminopyridine ($n = 2-4$) as Terminal Ligand

Oscar Castillo,[†] Antonio Luque,*[,†] Pascual Román,[†] Francesc Lloret,[‡] and Miguel Julve[‡]

Departamento de Química Inorgánica, Universidad del País Vasco, Apartado 644, E-48080 Bilbao, Spain, and Departament de Química Inorgànica, Facultat de Química, Universitat de València, Dr. Moliner 50, E-46100 Burjassot, València, Spain

Received March 27, 2001

The reaction of $M(ox)\cdot 2H_2O$ (M = Co(II), Ni(II)) or $K_2(Cu(ox)_2)\cdot 2H_2O$ (ox = oxalate dianion) with *n*-ampy (*n* = 2, 3, 4; *n*-ampy = *n*-aminopyridine) and potassium oxalate monohydrate yields one-dimensional oxalato-bridged metal(II) complexes which have been characterized by FT-IR spectroscopy, variable-temperature magnetic measurements, and X-ray diffraction methods. The complexes $M(\mu\text{-ox})(2\text{-ampy})_2$ (M = Co (**1**), Ni (**2**), Cu (**3**)) are isomorphous and crystallize in the monoclinic space group *C*2/*c* (No. 15), $Z = 4$, with unit cell parameters for **1** of $a = 13.885(2)$ Å, $b = 11.010(2)$ Å, $c = 8.755(1)$ Å, and $\beta = 94.21(2)°$. The compounds $M(\mu\text{-ox})(3\text{-ampy})_2\cdot 1.5H_2O$ (M = Co (**4**), Ni (**5**), Cu (**6**)) are also isomorphous and crystallize in the orthorhombic space group *Pcnn* (No. 52), $Z = 8$, with unit cell parameters for **6** of $a = 12.387(1)$, $b = 12.935(3)$, and $c = 18.632(2)$ Å. Compound $Co(\mu\text{-ox})(4\text{-ampy})_2$ (**7**) crystallizes in the space group *C*2/*c* (No. 15), $Z = 4$, with unit cell parameters of $a = 16.478(3)$ Å, $b = 5.484(1)$ Å, $c = 16.592(2)$ Å, and $\beta = 117.76(1)°$. Complexes $M(\mu\text{-ox})(4\text{-ampy})_2$ (M = Ni (**8**), Cu (**9**)) crystallize in the orthorhombic space group *Fddd* (No. 70), $Z = 8$, with unit cell parameters for **8** of $a = 5.342(1)$, $b = 17.078(3)$, and $c = 29.469(4)$ Å. All compounds are comprised of one-dimensional chains in which $M(n\text{-ampy})_2^{2+}$ units are sequentially bridged by bis-bidentate oxalato ligands with M···M intrachain distances in the range of 5.34−5.66 Å. In all cases, the metal atoms are six-coordinated to four oxygen atoms, belonging to two bridging oxalato ligands, and the endo-cyclic nitrogen atoms, from two *n*-ampy ligands, building distorted octahedral surroundings. The aromatic bases are bound to the metal atom in cis (**1**−**6**) or trans (**7**−**9**) positions. Magnetic susceptibility measurements in the temperature range of 2−300 K show the occurrence of antiferromagnetic intrachain interactions except for the compound **3** in which a weak ferromagnetic coupling is observed. Compound **7** shows spontaneous magnetization below 8 K, which corresponds to the presence of spin canted antiferromagnetism.

Introduction

Polynuclear oxalato-bridged complexes have been a focus of magnetic studies[1−3] for the last 25 years due to the capability of the oxalato ligand (ox) to adopt the bis-bidentate bridging mode together with its remarkable ability to mediate electronic effects between paramagnetic metal ions separated by more than 5 Å. A plethora of oxalato-bridged dinuclear complexes have been well characterized,[4−16] and intensive magnetostructural studies have analyzed, from both experimental[1,4,16] and theoretical[17−21] viewpoints, the structural and electronic factors (orbital topology, coordination polyhedron, donor atoms, and nature and substituents of the peripheral ligands) that govern the value of the magnetic coupling through oxalate. Recently,

* To whom correspondence should be addressed. E-mail: qipluara@lg.ehu.es. Fax: +34 944 648 500.
† Universidad del País Vasco.
‡ Universitat de València.

(1) Kahn, O. *Angew. Chem., Int. Ed. Engl.* **1985**, *24*, 834.
(2) Kahn, O. *Molecular Magnetism*; VCH: New York, 1993.
(3) Decurtins, S.; Schmalle, H. W.; Pellaux, R.; Fischer, P.; Hauser, A. *Mol. Cryst. Liq. Cryst. Sci. Technol., Sect. A* **1997**, *305*, 227.
(4) (a) Julve, M.; Verdaguer, M.; Kahn, O.; Gleizes, A.; Philoche-Levisalles, O. *Inorg. Chem.* **1983**, *22*, 368. (b) Julve, M.; Verdaguer, M.; Kahn, O.; Gleizes, A.; Philoche-Levisalles, O. *Inorg. Chem.* **1984**, *23*, 3808.
(5) Julve, M.; Faus, J.; Verdaguer, M.; Gleizes, A. *J. Am. Chem. Soc.* **1984**, *106*, 8306.
(6) Castro, I.; Calatayud, L.; Sletten, J.; Lloret, F.; Julve, M. *J. Chem. Soc., Dalton Trans.* **1997**, 811.
(7) Smekal, Z.; Thornton, P.; Sindelar, Z.; Klicka, R. *Polyhedron* **1998**, *17*, 1631.
(8) Castillo, O.; Muga, I.; Luque, A.; Gutiérrez-Zorrilla, J. M.; Sertucha, J.; Vitoria, P.; Román, P. *Polyhedron* **1999**, *18*, 1237.
(9) Felthouse, T. R.; Laskowski, E. J.; Hendrickson, D. N. *Inorg. Chem.* **1977**, *16*, 1077.
(10) Castro, I.; Faus, J.; Julve, M.; Mollar, M.; Monge, A.; Gutiérrez-Puebla, E. *Inorg. Chim. Acta* **1989**, *161*, 97.
(11) Gleizes, A.; Julve, M.; Verdaguer, M.; Real, J. A.; Faus, J.; Solans, X. *J. Chem. Soc., Dalton Trans.* **1992**, 3209.
(12) Vicente, R.; Escuer, A.; Ferretjans, J.; Stoeckli-Evans, H.; Solans, X.; Font-Bardía, M. *J. Chem. Soc., Dalton Trans.* **1997**, 167.
(13) Castro, I.; Faus, J.; Julve, M.; Gleizes, A. *J. Chem. Soc., Dalton Trans.* **1991**, 1937.
(14) Soto, L.; García-Lozano, J.; Escriva, E.; Beneto, M.; Dahan, F.; Tuchagues, J.; Legros, J. P. *J. Chem. Soc., Dalton Trans.* **1991**, 2619.
(15) Bencini, A.; Fabretti, C.; Zanchini, C.; Zannini, P. *Inorg. Chem.* **1987**, *26*, 1445.
(16) Glerup, J.; Goodson, P. A.; Hodgson, D. J.; Michelsen, K. *Inorg. Chem.* **1995**, *34*, 6255.
(17) Cabrero, J.; Ben Amor, N.; de Graaf, C.; Illas, F.; Caballol, R. *J. Phys. Chem. A* **2000**, *104*, 9983.
(18) Alvarez, S.; Julve, M.; Verdaguer, M. *Inorg. Chem.* **1990**, *29*, 4500.
(19) Cano, J.; Alemany, P.; Alvarez, S.; Verdaguer, M.; Ruiz, E. *Chem.—Eur. J.* **1998**, *4*, 476.
(20) Escuer, A.; Vicente, R.; Ribas, J.; Jaud, J.; Raynaud, B. *Inorg. Chim. Acta* **1994**, *216*, 139.

10.1021/ic0103401 CCC: $20.00
Published on Web 09/27/2001

the oxalate ion has allowed the construction of homo- and heterometallic two-[22] and three-dimensional[23] networks that have applications as molecular-based magnetic materials. Despite the great number of structurally characterized oxalato-bridged complexes, only a few examples of homometallic one-dimensional systems of formula $(M(\mu\text{-ox})(L)_x)_n$ (L = nitrogen-donor ligand or water) are known. Most of them are copper(II) systems whose magnetic studies reveal the occurrence of moderate[24,25] to weak[26,27] antiferromagnetic and even ferromagnetic intrachain couplings.[28−30]

As a contribution to this field and as a part of our magnetostructural work on metal−oxalate systems, we report herein the syntheses, crystal structures, and the magnetic behavior of a family of one-dimensional chains of general formula $M(\mu\text{-ox})(n\text{-ampy})_2\cdot x H_2O$, where M = Co(II), Ni(II), and Cu(II); $n = 2$ (**1**−**3**), 3 (**4**−**6**), and 4 (**7**−**9**); and $x = 0$ (**1**−**3** and **7**−**9**) and 1.5 (**4**−**6**). To our knowledge, similar oxalato-bridged one-dimensional complexes with M = Ni(II) or Co(II) have not been structurally characterized. Recently, a new family of polymers with a general formula $M(\mu\text{-ox})(\mu\text{-bpy})$ (M = Fe(II), Co(II), Ni(II), Zn(II); bpy = 4,4′-bipyridine) has been structurally and magnetically characterized, but the oxalato-bridged metal chains are joined by means of bidentate bpy ligands to form two-dimensional layered networks.[31] Coordination metal complexes with one-dimensional structures have long been investigated as molecular-based ferromagnets, conductors, and nonlinear optical materials. It is possible to modify the bulk magnetic, electronic, and optical properties of such materials by tailoring the molecules.[2,32−34] The distinctive properties of some one-dimensional materials, such as metamagnetism, spin glass, and spin liquid, are important in the fields of quantum mechanics and experimental and theoretical solid-state science.

Experimental Section

Materials. All chemicals were of reagent grade and were used as commercially obtained. Standard literature procedures were used to prepare the starting materials $Co(ox)\cdot 2H_2O$,[35a] $Ni(ox)\cdot 2H_2O$,[35a] and $K_2[Cu(ox)_2]\cdot 2H_2O$.[35b] Elemental analyses (C, H, N) were performed on a Perkin-Elmer 2400 microanalytical analyzer. Metal content was determined by absorption spectrometry.

Synthesis of $[Co(\mu\text{-ox})(2\text{-ampy})_2]$ (1). An aqueous solution (10 mL) of 2-ampy (0.200 g, 2.12 mmol) was added dropwise to a mixture (30 mL of water) of $Co(ox)\cdot 2H_2O$ (0.080 g, 0.44 mmol) and $K_2(ox)\cdot H_2O$ (0.500 g, 2.71 mmol). After filtration of the slight amount of insoluble material, the resulting almost red solution was allowed to evaporate at room temperature. Prismatic red crystals of **1** were separated from the mother liquor after 1 week,washed with cold water and diethyl ether, and dried in air. Yield: 70%. Anal. Calcd for $C_{12}H_{12}CoN_4O_4$: C, 43.00; H, 3.61; N, 16.72; Co, 17.58. Found: C, 42.86; H, 3.65; N, 16.62; Co, 17.66. Main IR features (cm^{-1}, KBr pellet): 3480s, 3355vs for ν(N−H); 3230m, 3210m, 3075w for ν(C−H); 1685vs, 1630vs for $\nu_{as}(CO_2)$; 1600vs, 1565s for (ν_{as}(C═C) + ν_{as}(C═N)); 1495vs, 1450s for ν(C−N); 1355m, 1335s, 1315m for $\nu_s(CO_2)$; 1260w, 1165m for δ(C−H); 1025w for ν_s(CO); 795m, 765s for $\delta(CO_2)$.

Synthesis of $[Ni(\mu\text{-ox})(2\text{-ampy})_2]$ (2). The preparation of **2** is analogous to that described for **1** but we used $Ni(ox)\cdot 2H_2O$ (0.080 g, 0.44 mmol), $K_2(ox)\cdot H_2O$ (0.200 g, 1.09 mmol), and 2-ampy (0.070 g, 0.74 mmol). Green polycrystalline powder of **2** was obtained after 3 days. Yield: 60%. Anal. Calcd for $C_{12}H_{12}NiN_4O_4$: C, 43.03; H, 3.61; N, 16.73; Ni, 17.52. Found: C, 42.98; H, 3.66; N, 16.69; Ni, 17.61. Main IR features (cm^{-1}, KBr pellet): 3485s, 3355vs for ν(N−H); 3230w, 3075w for ν(C−H); 1685vs, 1630vs for $\nu_{as}(CO_2)$; 1595vs, 1565s for (ν_{as}(C═C) + ν_{as}(C═N)); 1495s, 1450s for ν(C−N); 1355m, 1315m for $\nu_s(CO_2)$; 1260m, 1165m for δ(C−H); 1005w for ν_s(CO); 800m, 765m for $\delta(CO_2)$.

Synthesis of $[Cu(\mu\text{-ox})(2\text{-ampy})_2]$ (3). An aqueous solution (10 mL) of 2-ampy (0.094 g, 1.0 mmol) was added dropwise to an aqueous solution (30 mL) of $K_2[Cu(ox)_2]\cdot 2H_2O$ (0.354 g, 1.0 mmol) with continuous stirring. After filtration to remove any impurities, the solution was left undisturbed, and well-formed prismatic dark green crystals were deposited after 4 days. Crystals were collected by filtration, washed with cold water and diethyl ether, and dried in air. Yield: 40%. Anal. Calcd for $C_{12}H_{12}CuN_4O_4$: C, 42.42; H, 3.56; N, 16.49; Cu, 18.70. Found: C, 42.78; H, 3.62; N, 16.42; Cu, 18.40. Main IR features (cm^{-1}, KBr pellet): 3450s, 3350vs for ν(N−H); 1665s, 1635vs for $\nu_{as}(CO_2)$; 1620m for ν_{as}(C═N); 1590vs for ν_{as}(C═C); 1495s, 1450s for ν(C−N); 1360w, 1315m for $\nu_s(CO_2)$; 1265w, 1165m for δ(C−H); 1025m for ν_s(CO); 795m for $\delta(CO_2)$.

Synthesis of $[Co(\mu\text{-ox})(3\text{-ampy})_2]\cdot 1.5H_2O$ (4). The preparation of **4** is analogous to that described for **1** but we replaced 2-ampy with 3-ampy. Red prismatic single crystals of compound **4** were obtained after 3 days. Yield: 70%. Anal. Calcd for $C_{12}H_{12}CoN_4O_4\cdot 1.5H_2O$: C, 39.79; H, 4.17; N, 15.47; Co, 16.27. Found: C, 39.58; H, 4.22; N, 15.39; Co, 16.18. Main IR features (cm^{-1}, KBr pellet): 3520m for ν(O−H); 3430vs, 3350s, 3220sh for ν(N−H); 1675s, 1660s for

(21) (a) Román, P.; Guzmán-Miralles, C.; Luque, A.; Beitia, J. I.; Cano, J.; Lloret, F.; Julve, M.; Alvarez, S. *Inorg. Chem.* **1996**, *35*, 3741. (b) Escuer, A.; Vicente, R.; El Fallah, M. S.; Jaud, J. *Inorg. Chim. Acta* **1995**, *232*, 151.

(22) (a) Decurtins, S.; Schmalle, H. W.; Oswald, H. R.; Linden, A.; Ensling, J.; Gutlich, P.; Hauser, A. *Inorg. Chim. Acta* **1994**, *216*, 65. (b) Reiff, W. M.; Meda, L.; Kirss, R. U. *Mol. Cryst. Liq. Cryst. Sci. Technol., Sect. A* **1995**, *273*, 181. (c) Farrell, R. P.; Hambley, T. W.; Lay, P. A. *Inorg. Chem.* **1995**, *34*, 757. (d) Mathonière, C.; Nuttall, C. J.; Carling, S. G.; Day, P. *Inorg. Chem.* **1996**, *35*, 1201. (e) Carling, S. G.; Mathonière, C.; Day, P.; Malik, K. M. A.; Coles, S. J.; Hursthouse, M. B. *J. Chem. Soc., Dalton Trans.* **1996**, 1839. (f) Bhattacharjee, A.; Iijima, S.; Mitzutani, F. *J. Magn. Magn. Mater.* **1996**, *235*, 153. (g) Pellaux, R.; Schmalle, H. W.; Huber, R.; Fischer, P.; Hauss, T.; Ouladdiaf, B.; Decurtins, S. *Inorg. Chem.* **1997**, *36*, 2301. (h) Coronado, E.; Galán-Mascarós, J. R.; Goméz-García, C. J.; Ensling, J.; Gütlich, P. *Chem.−Eur. J.* **2000**, *6*, 552.

(23) (a) Decurtins, S.; Schmalle, H. W.; Schneuwly, P.; Oswald, H. R. *Inorg. Chem.* **1993**, *32*, 1888. (b) Decurtins, S.; Schmalle, H. W.; Schneuwly, P.; Ensling, J.; Gütlich, P. *J. Am. Chem. Soc.* **1994**, *116*, 9521. (c) Coronado, E.; Galán-Mascarós, J. R.; Giménez-Saiz, C.; Gómez-García, C. J.; Ruiz-Pérez, C.; Triki, S. *Adv. Mater.* **1996**, *6*, 737. (d) Decurtins, S.; Schmalle, H. W.; Pellaux, R.; Schneuwly, P.; Hauser, A. *Inorg. Chem.* **1996**, *35*, 1451. (e) Decurtins, S.; Schmalle, H. W.; Pellaux, R.; Huber, R.; Fisher, P.; Ouladdiaf, B. *Adv. Mater. (Weinheim, Ger.)* **1998**, *8*, 647. (f) Hernández-Molina, M.; Lloret, F.; Ruiz-Pérez, C.; Julve, M. *Inorg. Chem.* **1998**, *37*, 4131. (g) Andrés, R.; Gruselle, M.; Malézieux, B.; Verdaguer, M.; Vaissermann, J. *Inorg. Chem.* **1999**, *38*, 4637.

(24) Michalowicz, A.; Gired, J. J.; Goulon, J. *Inorg. Chem.* **1979**, *18*, 3004.

(25) Cavalca, L.; Chiesi-Villa, A.; Manfredotti, A.; Mangia, A.; Tomlinson, A. A. G. *J. Chem. Soc., Dalton Trans.* **1972**, 391.

(26) (a) Garaj, J.; Lagfelderova, H.; Lundgren, J.; Gazo, J. *Collect. Czech. Chem. Commun.* **1972**, *37*, 3181. (b) Girerd, J. J.; Kahn, O.; Verdaguer, M. *Inorg. Chem.* **1980**, *19*, 274.

(27) Kitagawa, S.; Okubo, T.; Kawata, S.; Kondo, M.; Katada, M.; Kobayashi, H. *Inorg. Chem.* **1995**, *34*, 4790.

(28) (a) Fitzgerald, W.; Foley, J.; McSweeney, D.; Ray, N.; Sheahan, D.; Tyagi, S. *J. Chem. Soc., Dalton Trans.* **1982**, 1117. (b) Oshio, H.; Nagashima, U. *Inorg. Chem.* **1992**, *31*, 3295.

(29) Suárez-Varela, J.; Domínguez-Vera, J. M.; Colacio, E.; Avila-Rosón, J. C.; Hidalgo, M. A.; Martín-Ramos, D. *J. Chem. Soc., Dalton Trans.* **1995**, 2143.

(30) Geiser, U.; Ramakrishna, B. L.; Willett, R. D.; Hulsbergen, F. B.; Reedijk, J. *Inorg. Chem.* **1987**, *26*, 3750.

(31) (a) Lu, J. Y.; Lawandy, M. A.; Li, J.; Yuen, T.; Lin, C. *Inorg. Chem.* **1999**, *38*, 2695. (b) Yuen, T.; Lin, C. L.; Mihalisin, T. W.; Lawandy, M. A.; Li, J. *J. Appl. Phys.* **2000**, *87*, 6001.

(32) Miller, J. S., Ed. *Extended Linear Chain Compounds*; Plenum: New York, 1982; Vol. 3.

(33) Delhaes, P., Drillon, M., Eds. *Organic and Inorganic Linear Dimensional Crystalline Materials*; NATO ASI Ser. 168; NATO: New York, 1989.

(34) Shen, H. Y.; Bu, W. M.; Gao, E. Q.; Liao, D. Z.; Jiang, Z. H.; Yan, S. P.; Wang, G. L. *Inorg. Chem.* **2000**, *39*, 396.

(35) (a)Remy, H. In *Treatise on Inorganic Chemistry*; VCH: Weinheim, Germany, 1956. (b) Kirschner, S. In *Inorganic Synthesis*; Rochow, E. G., Ed.; McGraw-Hill Book Co.: New York, 1960; Vol. VI.

Table 1. Single-Crystal Data and Structure Refinement Details[a]

	1	**3**	**4**	**6**	**7**	**8**	**9**
formula	$C_{12}H_{12}CoN_4O_4$	$C_{12}H_{12}CuN_4O_4$	$C_{12}H_{12}CoN_4O_4\cdot 1.5H_2O$	$C_{12}H_{12}CuN_4O_4\cdot 1.5H_2O$	$C_{12}H_{12}CoN_4O_4$	$C_{12}H_{12}NiN_4O_4$	$C_{12}H_{12}CuN_4O_4$
fw (g mol^{-1})	335.19	339.80	362.21	366.82	335.19	334.97	339.80
space group	*C*2/*c* (No. 15)	*C*2/*c* (No. 15)	*Pcnn* (No. 52)	*Pcnn* (No. 52)	*C*2/*c* (No. 15)	*Fddd* (No. 70)	*Fddd* (No. 70)
a (Å)	13.885(2)	13.472(2)	12.318(3)	12.387(1)	16.478(3)	5.342(1)	5.663(1)
b (Å)	11.010(2)	11.246(2)	13.014(2)	12.935(3)	5.484(1)	17.078(3)	16.589(2)
c (Å)	8.755(1)	8.694(2)	18.675(2)	18.632(2)	16.592(2)	29.469(4)	29.125(7)
β (deg)	94.21(2)	93.75(1)			117.76(1)		
V (Å^3)	1334.8(3)	1314.4(4)	2993.7(9)	2985.3(8)	1326.8(4)	2688.5(8)	2736.1(9)
Z	4	4	8	8	4	8	8
μ (cm^{-1})	13.1	16.8	11.8	15.8	13.2	14.7	16.2
D_{obsd} (g cm^{-3})	1.66(1)	1.71(1)	1.59(1)	1.62(1)	1.67(1)	1.64(1)	1.64(1)
D_{calcd} (g cm^{-3})	1.668	1.717	1.607	1.633	1.678	1.655	1.650
R^b	0.058	0.028	0.086	0.063	0.038	0.064	0.041
$R_w{}^c$	0.119	0.081	0.117	0.193	0.097	0.155	0.105

[a] Details in common: $T = 293(2)$ K, $\lambda = 0.71069$ Å, D_{obsd} measured in CCl_4/CH_2Br_2. [b] $R = \sum||F_o| - |F_c||/\sum|F_o|$. [c] $R_w = (\sum(w(F_o^2 - F_c^2)^2)/\sum(w(F_o^2)^2))^{1/2}$.

$\nu_{as}(CO_2)$; 1600vs, 1580s for (ν_{as}(C═N) + ν_{as}(C═C)); 1490w, 1445w for ν(C−N); 1385w, 1355w, 1310w for $\nu_s(CO_2)$; 1265w, 1195w for δ(C−H); 1025m for ν_s(CO); 810m, 795m for $\delta(CO_2)$.

Synthesis of [Ni(μ-ox)(3-ampy)$_2$]·1.5H$_2$O (5). The synthesis of **5** is analogous to that described for **2** but we used 3-ampy. A polycrystalline green sample of compound **5** was obtained after 3 days. Yield: 60%. Anal. Calcd for $C_{12}H_{12}NiN_4O_4\cdot 1.5H_2O$: C, 39.82; H, 4.18; N, 15.48; Ni, 16.22. Found: C, 39.77; H, 4.12; N, 15.53; Ni, 16.25. Main IR features (cm^{-1}, KBr pellet): 3520m for ν(O−H); 3420s, 3355s, 3225m for ν(N−H); 1680vs, 1660vs for $\nu_{as}(CO_2)$; 1600vs, 1580s for (ν_{as}(C═N) + ν_{as}(C═C)); 1490m, 1445w for ν(C−N); 1355w, 1315m for $\nu_s(CO_2)$; 1265w, 1200w for δ(C−H); 1025m for ν_s(CO); 800m for $\delta(CO_2)$.

Synthesis of [Cu(μ-ox)(3-ampy)$_2$]·1.5H$_2$O (6). This compound was prepared by following an analogous procedure to that for **3,** but we used the Cu(II) starting material and 3-ampy in the molar ratio of 1:2. After 1 week, green crystals of the complex **6** were obtained on standing at room temperature. Yield: 70%. Anal. Calcd for $C_{12}H_{12}CuN_4O_4\cdot 1.5H_2O$: C, 39.29; H, 4.12; N, 15.27; Cu, 17.32. Found: C, 38.97; H, 4.02; N, 15.32; Cu, 17.20. Main IR features (cm^{-1}, KBr pellet): 3520m for ν(O−H); 3430s, 3345s, 3220m for ν(N−H); 1670vs, 1635s for $\nu_{as}(CO_2)$; 1620s for ν_{as}(C═N); 1595vs for ν_{as}(C═C); 1490s, 1450s for ν(C−N); 1350w, 1305m for $\nu_s(CO_2)$; 1265w, 1200m for δ(C−H); 1060w, 1025w for ν_s(CO); 800m for $\delta(CO_2)$.

Synthesis of [Co(μ-ox)(4-ampy)$_2$] (7). Single crystals of **7** were prepared by the slow diffusion of a methanolic solution of 4-ampy (0.200 g, 2.12 mmol) into an aqueous solution of Co(ox)·2H$_2$O (0.080 g, 0.44 mmol) and K$_2$(ox)·H$_2$O (0.500 g, 2.71 mmol). Crystal growth was observed after 5 days. Yield: 80%. Anal. Calcd for $C_{12}H_{12}CoN_4O_4$: C, 43.00; H, 3.61; N, 16.72; Co, 17.58. Found: C, 42.99; H, 3.66; N, 16.68; Co, 17.64. Main IR features (cm^{-1}, KBr pellet): 3440s, 3345s, 3230m for ν(N−H); 1655m for $\nu_{as}(CO_2)$; 1625vs, 1605vs, 1560m for (ν_{as}(C═N) + ν_{as}(C═C)); 1515s, 1450w for ν(C−N); 1345m, 1315m, 1280w for $\nu_s(CO_2)$; 1060w, 1025m for ν_s(CO); 825m, 795w for $\delta(CO_2)$.

Synthesis of [Ni(μ-ox)(4-ampy)$_2$] (8). Single crystals of **8** were synthesized by the same procedure as that used for compound **7**. Light blue crystals were obtained after 1 week. Yield: 70%. Anal. Calcd for $C_{12}H_{12}NiN_4O_4$: C, 43.03; H, 3.61; N, 16.73; Ni, 17.52. Found: C, 42.97; H, 3.67; N, 16.81; Ni, 17.44. Main IR features (cm^{-1}, KBr pellet): 3435s for ν(N−H); 1655m for $\nu_{as}(CO_2)$; 1625vs, 1605vs, 1560m for (ν_{as}(C═N) + ν_{as}(C═C)); 1515s, 1445w for ν(C−N); 1345m, 1310m, 1280w for $\nu_s(CO_2)$; 1210m for δ(C−H); 1060w, 1010m for ν_s(CO); 825m, 795w for $\delta(CO_2)$.

Synthesis of [Cu(μ-ox)(4-ampy)$_2$] (9). Single crystals of **9** were prepared by the same procedure as that used for compound **7**, but we used an aqueous solution of K$_2$[Cu(ox)$_2$]·2H$_2$O. Crystals were obtained after 1 week. Yield: 70%. Anal. Calcd for $C_{12}H_{12}CuN_4O_4$: C, 42.42; H, 3.56; N, 16.49; Cu, 18.70. Found: C, 41.97; H, 3.41; N, 16.32; Cu, 18.97. Main IR features (cm^{-1}, KBr pellet): 3420s, 3335s, 3220m for ν(N−H); 1645s for $\nu_{as}(CO_2)$; 1630m for ν_{as}(C═N); 1605vs for ν_{as}(C═C); 1520m for ν(C−N); 1350m, 1305m for $\nu_s(CO_2)$; 1210m for δ(C−H); 1060w, 1025m for ν_s(CO); 795m for $\delta(CO_2)$.

Table 2. X-ray Powder Crystal Data for **2** and **5**

	2	**5**
formula	$C_{12}H_{12}NiN_4O_4$	$C_{12}H_{12}NiN_4O_4\cdot 1.5H_2O$
fw (g mol^{-1})	334.97	361.98
space group	*C*2/*c* (No. 15)	*Pcnn* (No. 52)
a (Å)	13.840(4)	12.336(8)
b (Å)	11.078(3)	12.903(8)
c (Å)	8.626(3)	18.585(9)
β (deg)	93.70(2)	
V (Å^3)	1319.7(4)	2958(3)
Z	4	8
D_{obsd} (g cm^{-3})	1.67(1)	1.63(1)
D_{calcd} (g cm^{-3})	1.685	1.625

The purity and homogenity of the polycrystalline samples of **1**−**9** used for physical measurements were checked by IR spectroscopy, elemental analysis, and comparison of the observed X-ray powder diffraction patterns with those generated from the single-crystal X-ray data.[36]

Physical Measurements. The IR spectra (KBr pellets) were recorded on a Nicolet 740 FT-IR spectrometer in the 4000−400 cm^{-1} spectral region. Magnetic measurements were performed on polycrystalline samples of the compounds with a Quantum Design SQUID susceptometer covering the temperature range of 2.0−300 K. The susceptibility data were corrected for the diamagnetism estimated from Pascal's tables,[37] the temperature-independent paramagnetism, and the magnetization of the sample holder.

X-ray Data Collection and Structure Determination. Data collections on single crystals were carried out at 293(2) K with an Enraf-Nonius CAD4 automatic four-circle diffractometer using graphite-monochromated Mo Kα radiation ($\lambda = 0.710\,69$ Å) and the $\omega-2\theta$ scan mode within the limits $2 \le 2\theta \le 60°$. Unit cell parameters and orientation matrix were determined by least-squares treatment of the setting angles of 25 well-centered reflections. No significant variation was observed in the intensities of the two reflections that were monitored periodically. Data were corrected for Lorentz and polarization effects. No absorption correction was applied. Neutral atom scattering factors and anomalous dispersion factors were taken from the literature.[38] Information concerning data collection and structural refinements is summarized in Table 1. The data reduction was done with the XCAD program.[39] The structures were solved by direct methods using the SIR

(36) Iron, K.; Jeitschko, W.; Parthe, E. *LAZY PULVERIX*; Laboratoire de Crystallographie aux Rayons-X, Universtité Genève: Switzerland, 1977.
(37) Earnshaw, A. *Introduction to Magnetochemistry*; Academic Press: London, 1968.
(38) *International Tables for X-ray Crystallography*; Kynoch: Birmingham, England, 1974; Vol. IV, p 99.

Table 3. Selected Bond Lengths (Å) and Angles (deg) for **1** and **3**[a]

	Co (**1**)	Cu (**3**)		Co (**1**)	Cu (**3**)
M(1)−O(1)	2.128(3)	1.990(1)	M(1)−N(11)	2.149(3)	2.031(1)
M(1)−O(2)	2.108(3)	2.379(1)			
O(1)−M(1)−O(2)	78.4(1)	76.18(4)	O(2)−M(1)−O(2a)	159.7(2)	155.04(6)
O(1)−M(1)−N(11)	89.2(1)	89.40(6)	O(2)−M(1)−N(11)	93.1(1)	92.40(5)
O(1)−M(1)−O(1a)	85.8(2)	86.96(7)	O(2)−M(1)−N(11a)	100.5(1)	104.61(5)
O(1)−M(1)−O(2a)	86.8(1)	85.72(5)	N(11)−M(1)−O(1a)	174.9(1)	176.22(5)
O(1)−M(1)−N(11a)	174.9(1)	176.22(5)	N(11)−M(1)−O(2a)	100.5(1)	104.61(5)
O(2)−M(1)−O(1a)	86.8(1)	85.72(5)	N(11)−M(1)−N(11a)	95.8(2)	94.25(8)
O(1a)−M(1)−O(2a)	78.4(1)	76.18(4)	O(2a)−M(1)−N(11a)	93.1(1)	92.40(5)
O(1a)−M(1)−N(11a)	89.2(1)	89.40(6)			

[a] Symmetry code: (a) $-x, y, {}^1/_2 - z$.

Table 4. Selected Bond Lengths (Å) and Angles (deg) in **4** and **6**

	Co (**4**)	Cu (**6**)		Co (**4**)	Cu (**6**)
M(1)−O(1)	2.124(5)	2.030(3)	M(1)−O(4)	2.165(6)	2.213(5)
M(1)−O(2)	2.077(6)	2.172(3)	M(1)−N(11)	2.125(6)	2.040(3)
M(1)−O(3)	2.083(6)	2.119(4)	M(1)−N(21)	2.115(7)	2.120(3)
O(1)−M(1)−O(2)	78.8(2)	79.3(1)	O(2)−M(1)−N(21)	98.0(2)	97.7(1)
O(1)−M(1)−O(3)	91.7(2)	89.7(1)	O(3)−M(1)−O(4)	78.4(2)	75.9(1)
O(1)−M(1)−O(4)	87.4(2)	86.9(1)	O(3)−M(1)−N(11)	94.7(2)	95.7(1)
O(1)−M(1)−N(11)	172.9(2)	173.3(1)	O(3)−M(1)−N(21)	90.4(3)	92.2(1)
O(1)−M(1)−N(21)	92.5(2)	93.2(1)	O(4)−M(1)−N(11)	90.9(2)	90.6(1)
O(2)−M(1)−O(3)	167.5(2)	165.5(1)	O(4)−M(1)−N(21)	168.7(3)	168.1(1)
O(2)−M(1)−O(4)	93.0(2)	94.0(1)	N(11)−M(1)−N(21)	90.4(2)	90.5(1)
O(2)−M(1)−N(11)	94.5(2)	94.7(1)			

Table 5. Main Bond Lengths (Å) and Angles (deg) in **7**[a]

Co(1)−O(1)	2.113(2)	Co(1)−O(2)	2.112(2)
Co(1)−N(11)	2.159(2)		
O(1)−Co(1)−O(2)	100.91(5)	O(2a)−Co(1)−N(11)	90.56(7)
O(1)−Co(1)−N(11)	90.43(7)	N(11)−Co(1)−(11a)	178.50(9)
O(1)−Co(1)−O(1a)	79.41(8)	O(2)−Co(1)−N(11a)	90.56(7)
O(1)−Co(1)−(2a)	178.96(6)	O(1a)−Co(1)−N(11)	90.72(7)
O(1)−Co(1)−N(11a)	90.72(7)	O(1a)−Co(1)−O(2a)	100.91(5)
O(1a)−Co(1)−O(2)	178.96(6)	O(1a)−Co(1)−N(11a)	90.43(7)
O(2)−Co(1)−N(11)	88.28(7)	O(2a)−Co(1)−N(11a)	88.28(7)
O(2)−Co(1)−O(2a)	78.78(8)		

[a] Symmetry code: (a) $-x, y, {}^1/_2 - z$.

92 program.[40] Full matrix least-squares refinements were performed on F^2, including all reflections and using SHELXL93.[41] The crystal structure of compound **9** shows remarkable disorder around a 2-fold axis affecting one oxalato ligand, and the positions of its atoms have been split into two (with multiplicities of 0.5) for a better structural resolution. All non-hydrogen atoms were refined anisotropically, except those belonging to the disordered oxalato ligands and the water of the 3-ampy complexes. All calculations were performed using the WinGX crystallographic software package.[42] The final geometrical calculations and the graphical manipulations were carried out with the PARST95[43] and PLATON[44] programs. X-ray powder diffraction data for compounds **2** and **5** were collected on a Philips X'PERT powder diffractometer with Cu Kα radiation in steps of 0.02 over the 2θ range of 5−60° with a fixed-time counting of 4 s at 25 °C. The patterns were indexed with the FULLPROF program.[45] Crystallographic data for compounds **2** and **5** are given in Table 2. Selected bond lengths and angles are listed in Tables 3−7.

(39) Harm, K.; Wocadlo, S. *XCAD*; CAD4 Data Reduction; University of Marburg: Germany, 1995.
(40) Altomare, A.; Cascarano, M.; Giacovazzo, C.; Guagliardi, A. *J. Appl. Crystallogr.* **1993**, *26*, 343.
(41) Sheldrick, G. M. *SHELXL93*: *Program for the Solution of Crystal Structures*; Universitat Göttingen: Germany, 1993.
(42) Farrugia, L. J. *WINGX*: *A Windows Program for Crystal Structure Analysis*; University of Glasgow: Great Britain, 1998.
(43) Nardelli, M. PARST95. *J. Appl. Crystallogr.* **1995**, *28*, 659.
(44) Spek, A. L. *Acta Crystallogr.* **1990**, *A46*, C34.
(45) Rodríguez-Carvajal, J. *FULLPROF*: *Program Rietveld Pattern Matching Analysis of Powder Patterns*; 1997.

Table 6. Selected Bond Lengths (Å) and Angles (deg) in **8**[a]

Ni(1)−O(1)	2.066(3)	Ni(1)−N(11)	2.099(8)
O(1)−Ni(1)−N(11)	90.6(1)	O(1c)−Ni(1)−N(11)	89.5(1)
O(1)−Ni(1)−O(1a)	178.9(3)	O(1a)−Ni(1)−O(1b)	98.4(2)
O(1)−Ni(1)−O(1b)	81.6(2)	O(1b)−Ni(1)−N(11b)	90.6(1)
O(1)−Ni(1)−N(11b)	89.5(1)	O(1b)−Ni(1)−O(1c)	178.9(3)
O(1)−Ni(1)−O(1c)	98.4(2)	O(1c)−Ni(1)−N(11b)	90.6(1)
O(1a)−Ni(1)−N(11)	90.6(1)	O(1a)−Ni(1)−N(11b)	89.5(1)
O(1b)−Ni(1)−N(11)	89.5(1)	O(1a)−Ni(1)−O(1c)	81.6(2)
N(11)−Ni(1)−N(11b)	180.0		

[a] Symmetry code: (a) ${}^1/_4 - x, {}^1/_4 - y, z$; (b) $x, {}^1/_4 - y, {}^1/_4 - z$; and (c) ${}^1/_4 - x, y, {}^1/_4 - z$.

Table 7. Selected Bond Lengths (Å) and Angles (deg) in **9**[a]

Cu(1)−O(1A)	2.052(4)	Cu(1)−N(11)	2.001(2)
Cu(1)−O(1B)	2.346(4)		
O(1A)−Cu(1)−O(1B)	75.9(1)	O(1Aa)−Cu(1)−O(1B)	104.1(1)
O(1A)−Cu(1)−N(11)	92.3(1)	O(1Aa)−Cu(1)−N(11)	92.3(1)
O(1A)−Cu(1)−O(1Aa)	175.4(2)	N(11)−Cu(1)−N(11b)	180.0
O(1A)−Cu(1)−O(1Ba)	104.1(1)	O(1Ba)−Cu(1)−N(11b)	89.3(1)
O(1A)−Cu(1)−N(11b)	87.7(1)	O(1Ba)−Cu(1)−N(11)	90.7(1)
O(1B)−Cu(1)−N(11)	90.7(1)	O(1Aa)−Cu(1)−O(1Ba)	75.9(1)
O(1B)−Cu(1)−N(11b)	89.3(1)	O(1Aa)−Cu(1)−N(11b)	87.7(1)
O(1B)−Cu(1)−O(1Ba)	178.5(2)		

[a] Symmetry code: (a) ${}^1/_4 - x, {}^1/_4 - y, z$; (b) $x, {}^1/_4 - y, {}^1/_4 - z$.

Results and Discussion

Description of the Structures. The main structural feature common to all compounds is the presence of $M^{II}(n\text{-ampy})_2^{2+}$ units bridged by bis-bidentate oxalato ligands leading to one-dimensional chains in which the metal atoms exhibit distorted octahedral MO_4N_2 surroundings.

[M(*μ*-ox)(2-ampy)$_2$] (M = Co (1), Ni (2), Cu (3)). Compounds **1**−**3** are isomorphous and crystallize in the monoclinic space group $C2/c$. The crystal structures of compounds **1** and **3** are comprised of *cis*-$(M(2\text{-ampy})_2)^{2+}$ units bridged sequentially by centrosymmetric oxalate anions to form zigzag polymeric chains which run parallel to the *c*-axis (Figure 1). The M···M separations across the bridging oxalato differ only slightly, being

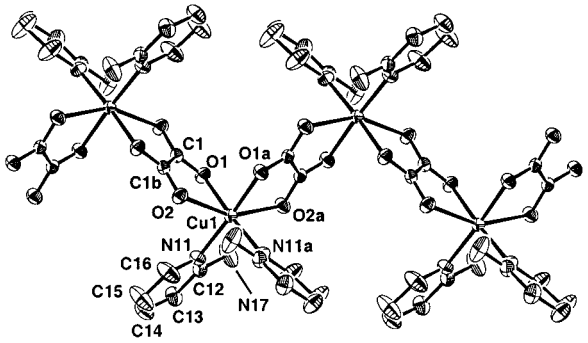

Figure 1. Perspective drawing of the polymeric chain of **3**. Thermal ellipsoids are drawn at the 50% probability level and the hydrogen atoms were omitted for simplicity.

5.500(1) Å in **1** and 5.629(1) Å in **3**. The metal atom, placed on a 2-fold axis, is coordinated to four oxygen atoms, from two bridging oxalato ligands, and the endo-cyclic nitrogen atoms, of two cis-arranged 2-ampy ligands. The two oxalato ligands around the metal atom are twisted by 79.2 and 72.0° for **1** and **3**, respectively.

The most significant difference between the two structures is the expected tetragonal Jahn−Teller distortion of the copper octahedron in **3**. The geometry around the cobalt(II) center can be best described as a slightly distorted octahedron. The Co−O distances are 2.128(3) and 2.108(3) Å, while the Co−N distance is 2.149(3) Å. These values are very close to those reported for oxalato-bridged polynuclear cobalt(II) complexes.[16,31] The coordination environment around the copper atom of **3** is an elongated octahedron with four short bonds formed by the endo-cyclic nitrogen atoms, from the two crystallographically related 2-ampy molecules (Cu−N: 2.031(1) Å), and two oxygen atoms, from two asymmetrically coordinated oxalato ligands (Cu−O: 1.990(1) Å). These atoms, which are reasonable planar (maximum deviation from the least-squares plane is 0.020(1) Å), define the equatorial plane. The copper atom is shifted by 0.02 Å from the equatorial plane. The axial coordination sites are occupied by the two remaining oxalate oxygen atoms, with a Cu−O bond distance (2.379(1) Å) that is markedly longer than the equatorial ones. The difference in the Cu−O distances (0.39 Å) is similar to those observed in other six-coordinated copper-(II) complexes.[13,27−29] The oxalato and the 2-ampy ligands form dihedral angles of 83.6 and 75.6°, respectively, with the equatorial coordination plane.

In both crystal structures, each chain in the unit cell is surrounded by four adjacent ones and they interact through N−H···O hydrogen bonds and offset face-to-face noncovalent interactions between the π-systems of the pyridine rings.

[M(μ-ox)(3-ampy)$_2$]·1.5H$_2$O (M = Co (4), Ni (5), Cu (6)). All three compounds are isomorphous and crystallize in the orthorhombic space group *Pcnn*. The crystal structures of compounds **4** and **6** are comprised of chains of *cis*-(M(3-ampy)$_2$)$^{2+}$ units joined sequentially by bis-bidentate oxalato ligands and two crystallographically independent solvated water molecules; one of them has the oxygen atom lying on a 2-fold axis. The coordination around the copper atom and a fragment of the polymeric structure of **6** showing the labeling scheme are shown in Figure 2. The metal(II) atoms are octahedrally surrounded by the endo-cyclic nitrogen atoms, of two cis-arranged 3-ampy ligands, and by four oxygen atoms, from two bridging oxalato ligands. Two different oxalato groups alternate regularly within the polymeric chain in contrast to what occurs in the 2-ampy complexes where all oxalato ligands are

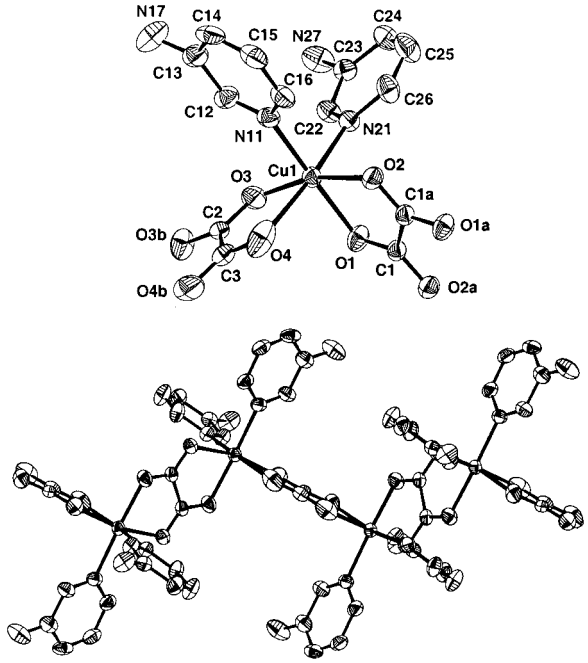

Figure 2. Coordination around the copper atom and a view of a fragment of the one-dimensional chain of compound **6**.

equivalent. One of the oxalate anions is centrosymmetric, whereas a 2-fold axis passes along the C−C bond of the second bridge. The dihedral angles between the oxalato mean planes are 88.7 and 86.2° for compounds **4** and **6**, respectively. The M···M distances through the oxalato bridges are 5.495(1) and 5.520(1) Å for **4** and 5.464(1) and 5.636(1) Å for **6**.

In the cobalt complex **4**, the Co−N (average value of 2.12 Å) and Co−O bond lengths (in the range of 2.077−2.165 Å) are comparable to those found in compound **1**. In the copper complex **6**, the copper environment shows two short [O(1) and N(11)], two medium [O(3) and N(21)], and two long distances [O(2) and O(4)] with a O(1)−Cu(1)−N(11) trans angle between the two short bonds of 173.3(1)°. These values represent an environment around the Cu(II) that is more akin to a rare example of "2 + 4" tetragonal compressed coordination or an elongated rhombic octahedral distortion resulting from a pseudo Jahn−Teller. In almost all the cases of observed Jahn−Teller "compression" examined in detail to date in the literature, the apparent compression is due to static/dynamic disorder of two of the possible axial elongations.[46,47] All our attempts to solve and refine the crystal structure of **6** considering disorder and/or a lower symmetry were unsuccessful. However, the values of the anisotropic displacement parameters of several atoms clearly indicate the existence of elongation accompanied by crystallographic disorder.

Similar to the 2-ampy complexes, the one-dimensional chains in **4** and **6** show a zigzag disposition with M···M···M angles of 116.6° (**4**) and 115.0° (**6**). However, it is worth noting that some subtle differences occur in the architecture of the chains. Whereas all metallic atoms of the chain in the 2-ampy complexes are coplanar, the metallic atoms in compounds **4** and

(46) (a) Falvello, L. R. *J. Chem. Soc., Dalton Trans.* **1997**, 4463. (b) Astley, T.; Headlam, H.; Hitchman, M. A.; Keene, F. R.; Pilbrow, J.; Stratemeier, H.; Tiekink, E. R. T.; Zhong, Y. C. *J. Chem. Soc., Dalton Trans.* **1995**, 3809. (c) Stratemeier, H.; Wagner, B.; Krausz, E. R.; Linder, R.; Schmidtke, H. H.; Pebler, J.; Hatfield, W. E.; ter Haar, L.; Reinen, D.; Hitchman, M. A. *Inorg. Chem.* **1994**, *33*, 2340.

(47) Atanasov, M.; Hitchman, M. A.; Hoppe, R.; Murray, K. S.; Moubaraki, B.; Reinen, D.; Stratemeier, H. *Inorg. Chem.* **1993**, *32*, 3397.

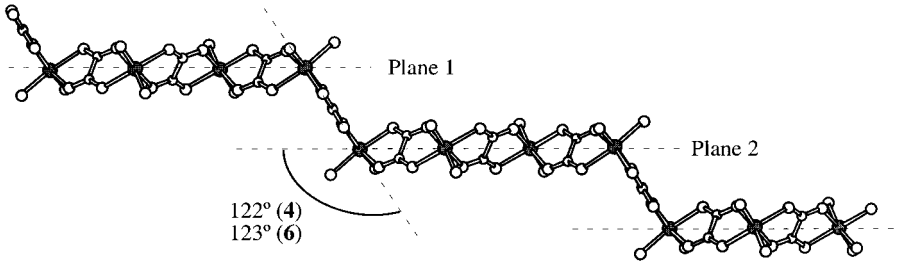

Figure 3. Arrangement of the polymeric chain of compounds **4** and **6**. Noncoordinated atoms of the terminal ligands were omitted for clarity.

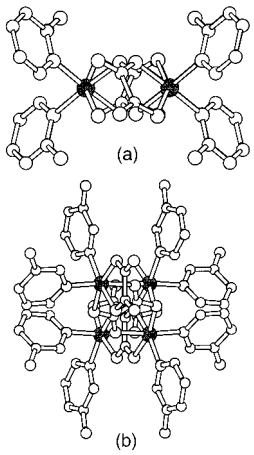

Figure 4. Ball and stick drawings showing the different arrangements of the zigzag chains of (a) compound **3** and (b) compound **6**.

6 form parallel fragments of four coplanar metal(II) ions. The dihedral angles between one of these fragments and the bridging oxalato ligand are 122 and 123° for **4** and **6**, respectively (Figure 3). The outer of 2-ampy and 3-ampy chains is also different as can be observed in Figure 4. The result is the presence of bulkier chains in **4** and **6** which leads to a less effective packing, with holes which are occupied by crystallization water molecules. Indeed, the density values of 3-ampy complexes (**4**−**6**) are smaller than those for 2-ampy complexes (**1**−**3**).

In the crystal structures of **4** and **6**, the one-dimensional chains are held together by means of offset face-to-face $\pi-\pi$ interactions, between the aromatic rings of the 3-ampy ligands, and a three-dimensional network of hydrogen-bond contacts, involving the exo-cyclic nitrogen and the oxygen atoms of the axiosymmetric oxalato ligand. The crystallization water molecules are inserted into the hydrophilic holes generated by the oxalato oxygen atoms and the exo-cyclic nitrogen atoms, and they interact by means of hydrogen-bonding interactions of the type $N-H\cdots O_w$. Although the hydrogen atoms of the water molecules could not be found from the difference Fourier map due to the modest quality of the single crystal, the observed $O_w\cdots O/O_w$ contact distances suggest a more extensive hydrogen-bond network involving the water molecules.

[M(μ-ox)(4-ampy)$_2$] (M = Co (7), Ni (8), Cu (9)). Compound **7** crystallizes in the monoclinic space group *C*2/*c*, whereas the nickel (**8**) and copper (**9**) complexes crystallize in the orthorhombic space group *Fddd*. Their crystal structures consist of neutral linear chains of metal(II) ions linked by bis-bidentate oxalato bridges, and the octahedral coordination of the metal centers is completed by two pyridinic nitrogen atoms from two crystallographically related 4-ampy molecules which, in contrast to the above-described complexes, show a trans arrangement. Although the polymeric chains of the three complexes are similar, they show some significant differences. The polymeric chain of the cobalt complex **7** (Figure 5) shows

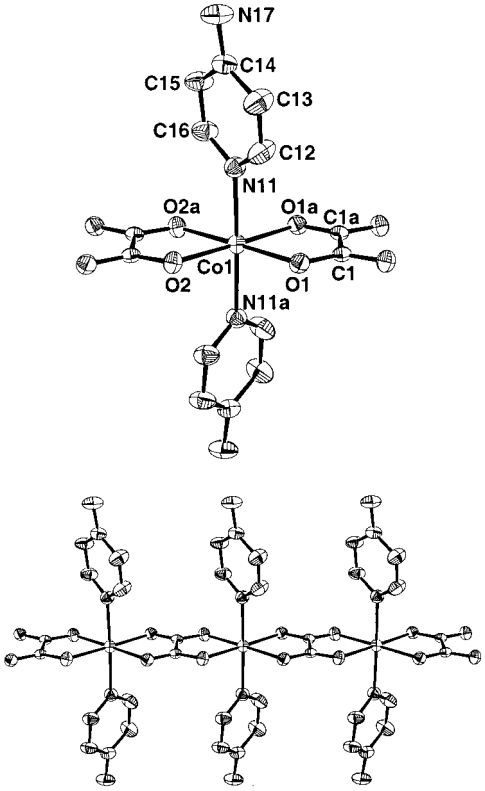

Figure 5. Coordination environment of the cobalt atom and a view of a fragment of the chain in compound **7**.

a C_2 symmetry with one 2-fold axis, along the crystallographic *b*-axis, passing through the metal centers and the middle of the C−C bond of the oxalato ligand. The Co···Co distance through the bridge is 5.484(1) Å. The oxalato ligand is essentially planar, and the two $-CO_2$ groups are twisted by 1.8°. The aromatic ligand is slightly tilted with respect to the planar ox−Co−ox framework at a dihedral angle of 83.6°. The Co−N bond distance (2.159(2) Å) is somewhat longer than those for Co−O (2.113(2), 2.112(2) Å). The trans N−Co−N angle is 178.50-(9)°, and the main distortion from the octahedral symmetry of the metal environment is due to the bite angles of the bis-bidentate oxalato ligand (79.41(8) and 78.78(8)°).

The polymeric chains of the compound **8** grow along the crystallographic *a*-axis and show a higher symmetry. The hexacoordinated nickel atoms and the oxalato bridges are placed in D_2 symmetry points. An ORTEP plot of the chain is shown in Figure 6. The four equivalent Ni−O equatorial distances are shorter than the two equal Ni−N axial distances (2.066(3) vs 2.099(8) Å). The trans N(11)−Ni−N(11b) angle is linear, and the aromatic rings are perpendicular to the nickel−oxalato framework. The oxalato ligand is almost planar, the two $-CO_2$ groups are twisted by 1.8°, and the bite angle is 81.6°. The distance between the two nickel atoms through the bridging oxalato is 5.342(1) Å (the *b*-axis length).

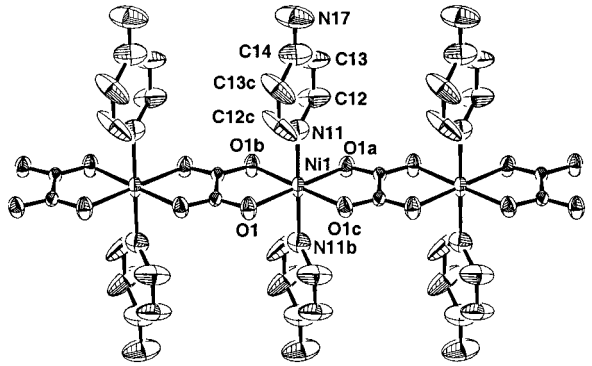

Figure 6. View of a fragment of the linear chain of compound **8**.

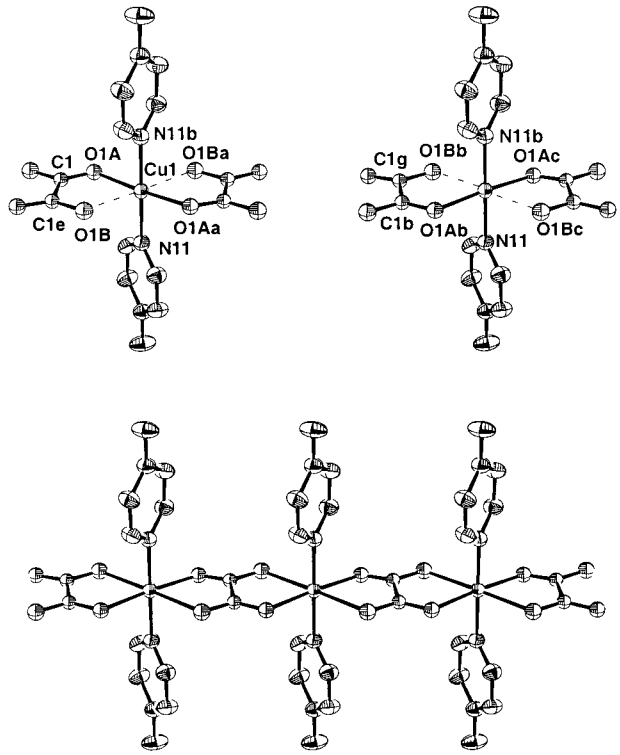

Figure 7. Perspective drawings of the coordination around copper atom showing the two disordered positions of oxalato ligands and a view of a fragment of the chain of compound **9**.

The polymeric chain of **9** is similar to that described for compound **8**. The copper atoms are also placed in a D_2 symmetry point, but the axiosymmetric oxalato ligand is disordered in two positions related by two 2-fold axes. An ORTEP plot of the coordination sphere around the metal center, showing the two disordered positions of the oxalato ligand and the arrangement of the polymeric chain in **9**, is shown in Figure 7. The CuO_4N_2 chromophore must be described as an usual elongated tetragonal octahedron with four short distances (Cu−N(11), 2.001(2) Å; Cu−O(1A), 2.051(4) Å) and two long ones (Cu−O(1B), 2.346(4) Å). The value of the intrachain copper−copper distance (5.663(1) Å) is larger than that reported for the complexes Cu(μ-ox)·1/3H_2O (EXAFS data, 5.14 Å)[24] and Cu_2-(μ-ox)$_2$(pyrazine)$_3$ (5.29 Å),[27] but it is shorter than that found in Cu(μ-ox)$(NH_3)_2$·2H_2O (5.78 Å).[26] In all of them, the two oxalato bridges are also trans coordinated to the copper atom. It should be noticed that as far as we know, these compounds are the only structurally characterized examples of linear oxalato-bridged metal(II) chains although the pyrazine-containing complex is actually a two-dimensional network in which the oxalato-bridged copper(II) chains are joined by bis-monodentate pyrazine ligands.

Each chain within a unit cell of the compounds **7**−**9** is interconnected to the nearest four units by means of H bonds involving the oxalato oxygen and the *exo*-amino groups of the aromatic ligands. In contrast to 2- and 3-ampy complexes, no face-to-face $\pi-\pi$ stacking interactions between the aromatic rings have been found in the 4-ampy compounds.

We would like to finish the structural description of these compounds with a brief analysis of the relation between the position of the amino substituent in the aromatic rings and the arrangement of the peripheral ligands. At first sight, the adoption of the cis coordination in the 2- and 3-ampy complexes may be considered to be due to the minimization of steric hindrances between the substituent and the oxalato−metal framework. The lack of geometrical constraints in the 4-ampy complexes is due to the fact that the amino group is placed on the opposite side of the pyridine-nitrogen atom, and so, a trans coordination around the metal centers is observed. This arrangement is also found in the polymeric compounds [Cu_2(μ-ox)$_2$(pyrazine)$_3$][27] and [Cu(μ-ox)$(NH_3)_2$]·2H_2O.[26] Recently, we have reported the crystal structure of the polymeric compound [Cu(μ-1,2-CO_3)-(4-ampy)$_2$]·H_2O,[48] where the aromatic molecules are also trans coordinated to the metal ions and lie above and below the planar carbonato−copper(II) skeleton. On the contrary, for the [Cu-(μ-ox)(py)$_2$][29] complex, the pyridine molecules are cis coordinated around the copper atoms. It remains true, however, that this complex was accidentally obtained from the breakdown of a starting copper complex containing two cis-coordinated pyridine molecules. In addition, face-to-face aromatic $\pi-\pi$ interactions are present in the crystal packing of the pyridine compound, which do not occur in all the above cited compounds with a trans arrangement of the aromatic rings. All our attempts to obtain a similar compound directly from an oxalate−metal-(II)−pyridine system were unsuccessful. It is most likely that steric effects dictate the arrangement of the terminal ligands, but packing forces such as aromatic-ring stacking ($\pi-\pi$ interactions) and hydrogen bonds are also relevant factors, and they could be crucial in the determination of the arrangement that we observe in the compounds described in this work.

Magnetic Properties. The magnetic properties of the cobalt-(II) complexes, in the form of χ_M (the molar magnetic susceptibility per metal atom) vs T at a magnetic field of 1000 G, are represented in Figure 8. The χ_M curves increase when the compounds are cooled until a maximum is reached at 27 (**1**), 24 (**4**), and 18 K (**7**) with values of 2.93×10^{-2}, 3.46×10^{-2}, and 3.59×10^{-2} cm^3 mol^{-1}, respectively, and then decrease very quickly. The $\chi_M T$ curves exhibit a continuous decrease upon cooling. This behavior is indicative of a moderate antiferromagnetic coupling between the cobalt(II) centers through the bridging oxalato ligand. The room-temperature $\chi_M T$ values (2.731 (**1**), 2.934 (**4**), and 2.851 cm^3 mol^{-1} K (**7**)) are much larger than the spin-only value of 1.875 cm^3 mol^{-1} K for an uncoupled high-spin cobalt(II) ion (with $S = {}^3/_2$) indicating that an important orbital contribution is involved. The temperature dependence of the magnetic susceptiblity of the three compounds was also investigated under an applied magnetic field of $H = 50$ G. The shape of the χ_M curves at 50 and 1000 G is essentially the same for the compounds **1** and **4**. But it is substantially different in the low-temperature range (Figure 9) for the compound **7**. When the sample was cooled within the 50 G field, the magnetic susceptibility shows an abrupt increase

(48) Sertucha, J.; Luque A.; Castillo, A.; Román, P.; Lloret, F.; Julve, M. *Inorg. Chem. Commun.* **1999**, *2*, 14.

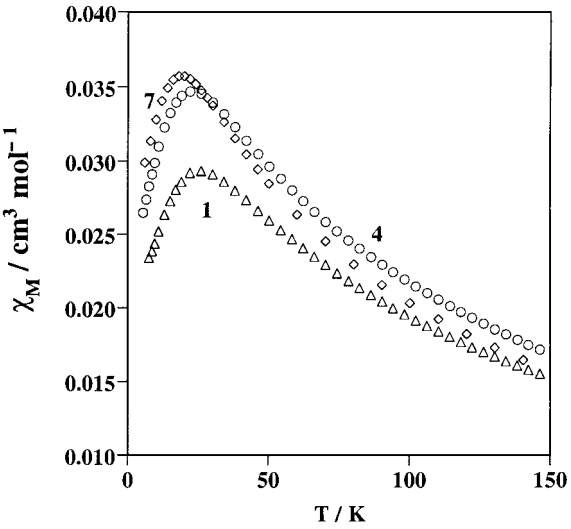

Figure 8. Plots of the thermal dependence of χ_M for the cobalt(II) compounds (△ (**1**), ○ (**4**), and ◇ (**7**)), experimental data.

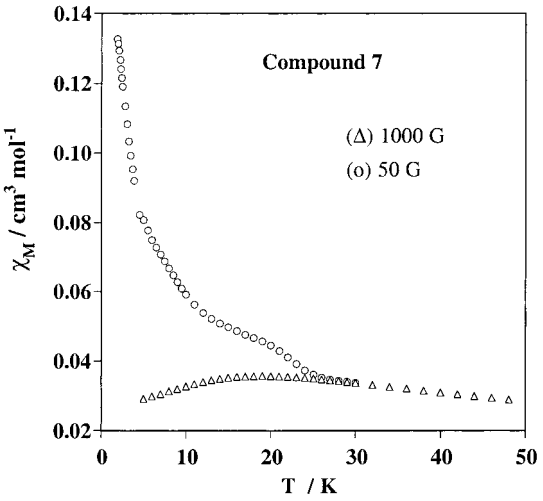

Figure 9. Thermal dependence of χ_M for compound **7** in applied magnetic fields of 50 G (○) and 1000 G (△) in the low-temperature region.

at 8 K, and below this temperature it becomes field dependent. This fact suggests a ferromagnetic phase transition. The ordering temperature was confirmed by the measurement of both the in-phase and out-of-phase components of the ac magnetic susceptibility. Further support for this comes from magnetization vs applied magnetic field plots which at temperatures above 8 K are linear and extrapolate to zero magnetization at zero applied field. Below this temperature, the plots are not linear and extrapolate to yield net magnetization at zero applied field. The highest magnetization reached at 2 K and 50 000 G is 1430 cm^3 G mol^{-1}, significantly below the theoretical saturation magnetization of 16 755 cm^3 G mol^{-1}.[49] The magnetic hysteresis loop for compound **7** measured at 2 K is characteristic of a soft magnet with a small coercive field of 180 G and a remnant magnetization of 6 cm^3 G mol^{-1}. We interpret the magnetic properties of **7** as a consequence of canted spin antiferromagnetism leading to weak ferromagnetism at low temperatures.[2] It is well-known that the occurrence of spin canting can be due to either (i) magnetic anisotropy or (ii) antisymmetric magnetic exchange.[50] A spin canting phenomenon owing to the magnetic anisotropy in compound **7** seems to be precluded owing to the absence of the systematic alternation of the relative orientation of neighboring metal chromophores, which is characteristic in some of these systems.[51] Consequently, the observed spin canting may be attributed to the antisymmetric magnetic exchange that tends to orient the neighboring spins perpendicular each to other. This interaction vanishes when the molecular entity is centrosymmetric and also when its molecular symmetry is C_{nv} ($n \geq 2$) or higher, with the n-fold axis joining the interacting centers.[2] The polymeric chain of **7** shows a C_2 symmetry with one 2-fold axis passing through the metal atoms, but this axis does not relate two neighboring CoO_4N_2 chromophores. In conclusion, in the high-temperature region, antiferromagnetic coupling between metal centers via oxalato ligands within the extended one-dimensional chains leads to a canted spin structure. Below 8 K, three-dimensional magnetic ordering of the uncompensated spin occurs. A mechanism for this could involve interactions via the H-bonding network that links the chains. The presence of canted antiferromagnetic orderings has been also observed in the two-dimensional complexes [M(μ-ox)(μ-bpy)] (M = Fe(II), Co(II)).[31]

Our attempts to evaluate the exchange coupling for compounds **1** and **4**, by using the classical spin Heisenberg chain model[52] with $S = {}^3/_2$, were unsuccessful. The calculated χ_M curves do not match the experimental data in the vicinity of the maximum, with the position of the theoretical maximum being shifted toward higher temperatures with respect to that of the experimental one. The values of the magnetic coupling J thus obtained (-9.8 and -8.9 cm^{-1} for **1** and **4**, respectively) are overestimated, and the orbital contribution to the magnetic moment has to be taken into account. Reports on magnetic studies of some chain and layered six-coordinated cobalt(II) compounds show that, at low temperature, these magnetic systems behave as collections of Ising chain $S = {}^1/_2$ effective spins coupled by not only ferromagnetic but also antiferromagnetic interactions.[53] The Ising model[54] is restricted to the temperature range where only the ground Kramers doublet is thermally populated ($T < 30$ K). This is not dramatic if $|J|$ is very small. Most of the information may then be deduced from low-temperature magnetic data. But the low-temperature magnetic data are much less informative when J is of the same order of magnitude as the energy gap between the two Kramers doublets. All our attempts to obtain a satisfactory fit of the experimental data using the Ising model were unsuccessful. However, it is interesting to notice that the magnetism curves for the complexes **1** and **4** are similar to those reported for dimeric oxalato-bridged cobalt(II) complexes with N-tetradentate terminal ligands which show J values from -8 to -12 cm^{-1}.[16] Oxalato-bridged cobalt(II) complexes typically have exchange coupling of up to -15 cm^{-1}, and there are no known examples where the oxalate mediates a ferromagnetic interaction.[16,55]

(49) Carling, R. L. *Magnetochemistry*; Springer-Verlag: Berlin, 1986; pp 7−9.

(50) Miller, J. S.; Calabrese, J. C.; McLean, R. S.; Epstein A. J. *Adv. Mater. (Weinheim, Ger.)* **1992**, *4*, 498.

(51) Rettig, S. J.; Thompson, R. C.; Trotter, J.; Xia, S. *Inorg. Chem.* **1999**, *38*, 1360.

(52) Fisher, M. E. *Am. J. Phys.* **1964,** *32*, 343.

(53) (a) De Munno, G.; Poerio, T.; Julve, M.; Lloret, F.; Viau, G. *New J. Chem.* **1998**, 299. (b) Zhang, W.; Jeitler, J. R.; Turnbull, M. M.; Landee, C. P.; Wei, M.; Willet, R. D. *Inorg. Chim. Acta* **1997**, *256*, 183.

(54) Fisher, M. E. *J. Math. Phys.* **1963**, *4*, 124.

(55) (a) Price, D. J.; Powell, A. K.; Wood, P. T. *J. Chem. Soc., Dalton Trans.* **2000**, 3566. (b) Lukin, J. A.; Simuzu, S.; Vanderven, N. S.; Friedberg, S. A. *J. Magn. Magn. Mater.* **1995**, *140*, 1669. (c) Sledzinska, I.; Musarik, A.; Fischer, P. *J. Phys. C: Solid State Phys.* **1988**, *21*, 5273. (d) Van Kralingen, C. G.; Van Ooijen, J. A. C.; Reedijk, J. *Transition Met. Chem.* **1978**, *3*, 90.

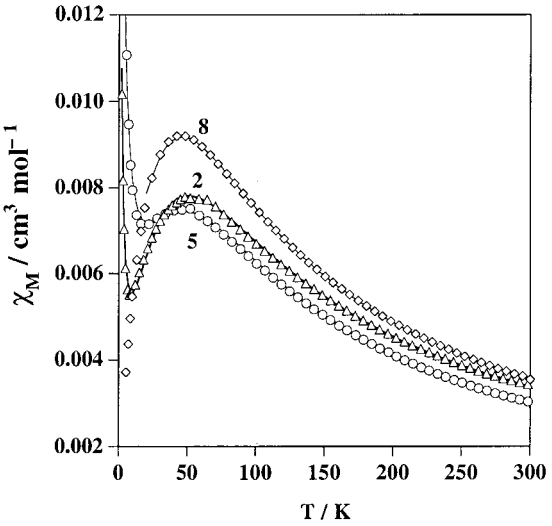

Figure 10. Plots of the thermal dependence of χ_M for the nickel(II) compounds (△ (**2**), ○ (**5**), and ◇ (**8**)), experimental data; (–) best theoretical fit (see text).

Table 8. Best-Fit Values for Ni(II) and Cu(II) Compounds

	compd	J (cm^{-1})	g	ρ (%)	R x 10^5
Ni	**2**	−28.4	2.14	2.8	3.7
	5[a]	−30.2/−26.8	2.16	1.5	4.5
	8	−24.4	2.20		9.6
Cu	**3**	+2.0	2.16		4.0
	6[a]	−44.5/−1.3	2.13	1.4	3.1
	9	−1.1	2.10		4.1

[a] J: $J/\alpha J$.

The thermal dependence of the molar magnetic susceptibility, χ_M, of nickel complexes (Figure 10) is characteristic of antiferromagnetic interactions between the nickel(II) centers. The χ_M value increases as the temperature is lowered until a maximum is reached (T_{max} = 50 (**2**), 48 (**5**) and 44 K (**8**)) and finally decreases very quickly. Below 20 K, the χ_M curves of the 2- and 3-ampy complexes increase due to the presence of a small amount of paramagnetic impurities. Taking into account the structural features, the magnetic data were fitted by numerical expressions proposed for $S = 1$ chains with uniform[56] (**2**, **8**) and alternate[57] (**5**) antiferromagnetic interactions. The results of the best-fits are listed in the Table 8. The percentage of paramagnetic impurities per mole of nickel atoms (assuming that the molecular weight of the impurity is the same as that of the investigated compound) is given by ρ, and R is the agreement factor defined as $R = \sum_i((\chi_M)_{obs}(i) - (\chi_M)_{calc}(i))^2/\sum_i((\chi_M)_{obs}(i))^2$. The χ_M curve for compound **8** does not show the presence of any paramagnetic impurities, and in contrast to that predicted by the theoretical model, the experimental values tend to zero when T approaches zero. A good fit of the magnetic data for this compound is possible only up to a temperature near the maximum of χ_M, because neither the single-ion anisotropy nor the Haldane gap effect[58] are taken into account in the magnetic model. Previous magnetostructural studies of dinuclear oxalato-bridged Ni(II) complexes[21] have revealed that J can vary from −22 to −40 cm^{-1}. The magnitude of the exchange coupling constant is strongly dependent on the nature of the donor atoms in the peripheral ligands: the less electronegative they are, the greater is the antiferromagnetic coupling. The observed values of J for the compounds **2**, **4**, and **6** compare well with that reported for the dimer $[Ni_2(\mu\text{-ox})(acac)(tmen)_2]$ (acac = acetylacetonate; tmen = *N*,*N*,*N*′,*N*′-tetramethylethylenediamine; J = −28.6 cm^{-1})[59] that also shows a NiO_4N_2 chromophore, but the antiferromagnetic couplings are somewhat lower than those found for nickel−oxalato dinuclear systems in which the nickel(II) atoms are placed in NiO_2N_4 environments (J ranges from −32 to −40 cm^{-1}). Other features such as the basicity of the terminal ligand, the Ni−O(ox) bond lengths, and the structural distortions (especially those involving deviations from the planarity of the metal ion with respect to the mean plane of the bridging ligand or equatorial plane) can play a key role in the fine-tuning of the exchange coupling.

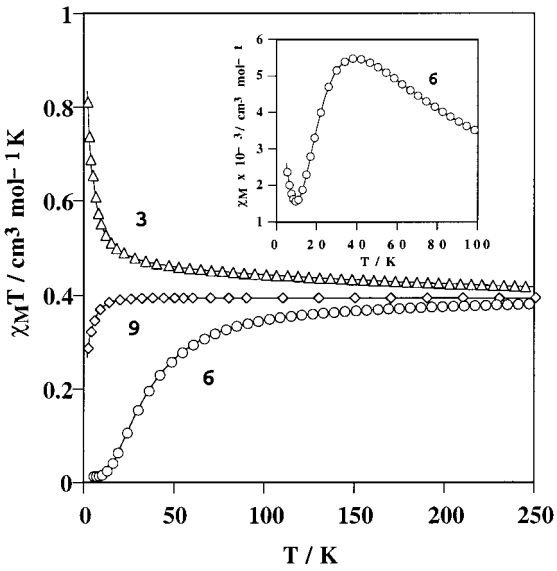

Figure 11. Plots of the thermal dependence of $\chi_M T$ for the copper(II) compounds (△ (**3**), ○ (**6**), and ◇ (**9**)), experimental data; (–) best theoretical fit (see text). Inset: thermal variation of the molar magnetic susceptibility for compound **6**.

The temperature dependence of the $\chi_M T$ product (χ_M is the magnetic susceptibility per copper atom) for compounds **3**, **6**, and **9** is shown in Figure 11. At room temperature, the $\chi_M T$ values are 0.416 (**3**), 0.394 (**6**), and 0.409 (**9**) cm^3 mol^{-1} K. Upon cooling, the $\chi_M T$ curve for **3** increases continuously up to a value of 0.834 cm^3 mol^{-1} K at 2.0 K. This trend of $\chi_M T$ is indicative of the predominance of ferromagnetic interactions in this compound. For **6,** $\chi_M T$ decreases markedly upon cooling and it attains a value of 0.014 cm^3 mol^{-1} K at 12 K. Below this temperature, this value remains practically constant owing to the presence of a small amount of paramagnetic impurities. The χ_M curve of **6** shows a maximum at 40 K, indicating that significant antiferromagnetic coupling is involved. Upon cooling, the value of $\chi_M T$ for **9** decreases smoothly until approximately 60 K. At lower temperatures, $\chi_M T$ decreases at a faster rate, reaching a value of 0.268 cm^3 mol^{-1} K at 2.0 K. These features indicate the occurrence of weak antiferromagnetic exchange interactions between the copper ions in **9**. No maximum of magnetic susceptibility is observed in this case.

Taking into account that **3** and **9** are regular chains, their magnetic data were successfully fitted by numerical expressions proposed for uniform copper(II) chains with ferro- (**3**)[60] and

(56) (a) Weng, C. Y. Ph.D. Thesis, Carnegie Institute of Technology, 1968. (b) Meyer, A.; Gleizes, A.; Girerd, J. J.; Verdaguer, M.; Kahn, O. *Inorg. Chem.* **1982**, *21*, 1729.
(57) Borras-Almenar, J. J.; Coronado, E.; Curely, J.; Georges, R. *Inorg. Chem.* **1995**, *34*, 2699.
(58) (a) Haldane, F. D. M. *Phys. Lett.* **1983**, *A93*, 464. (b) Haldane, F. D. M. *Phys. Rev. Lett.* **1983**, *50*, 1153.
(59) Yamada, K.; Fukuda, Y.; Kawamoto, T.; Kushi, Y.; Mori, W.; Unuora, K. *Bull. Chem. Soc. Jpn.* **1993**, *66*, 2758.
(60) Baker, G. A.; Rushbrooke, G. S. *Phys. Rev.* **1964**, *135*, 1272.

antiferromagnetic (**9**)[61] intrachain interactions derived through the Hamiltonian $H = -J\sum S_iS_{i+1}$. Given that two crystallographically independent bridging oxalato ligands alternate regularly in **6**, its magnetic data were fitted to an antiferromagnetic Heisenberg $S = {}^1/_2$ alternating chain model[2] derived through the Hamiltonian $H = -J\sum[S_{2i}S_{2i-1} + \alpha S_{2i}S_{2i+1}]$ (α is the alternating parameter and $S_{2i-1} = S_{2i} = S_{2i+1} = 1/2$). The results of the least-squares fits for **3**, **6**, and **9** are shown in Table 8. The calculation for **6** was limited to the data ranging from 15 to 300 K, because the theoretical results of the alternating chain model are unreliable for values of $kT/|J|$ less than 0.25.

In previous experimental and theoretical studies of oxalato-bridged copper complexes,[17−19] it has been found that the exchange interactions between the metal ions are governed by the magnitude of the overlap between the metal-centered magnetic orbitals (a $d_{x^2-y^2}$ type orbital in square pyramidal or elongated octahedral geometries) and the symmetry-adapted highest occupied molecular orbitals (HOMOs) (σ symmetry) of the oxalato ligand. In fact, the value of the exchange coupling (J) in a copper(II) dimer is decomposed into two terms, of which one is antiferromagnetic (J_{AF}) and the other is ferromagnetic (J_F) according to $J = J_{AF} + J_F$.

The magnitude of the antiferromagnetic term is essentially governed by the square of the integral overlap between the magnetic orbitals, whereas that of the ferromagnetic one is very small for extended bridges such as the oxalato bridge.[62] Strong antiferromagnetic coupling (J ranging from -260 to -400 cm^{-1})[4,5,8,11,15,18] results when the short copper−ligand bonds are coplanar with the bridging ligand. In such a case, the singly occupied molecular orbitals (SOMOs) are built up from d orbitals that are well oriented to interact with the bridging ligand. The smallest interaction occurs when one of copper-bridge distances is long (i.e., oxalato bridge is asymmetrically coordinated). In this case, the two metal-centered magnetic orbitals are parallel but perpendicular to the bridging oxalato ligand

Chart 1

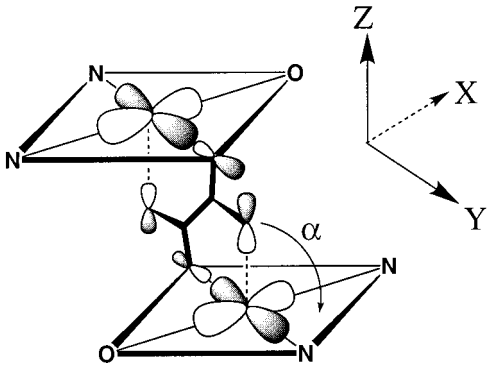

(Chart 1), the interaction between the highest energy d orbitals through the bridge is poor, and a weak antiferromagnetic coupling results. Even so, depending on the α angle the overlap can be zero (accidental orthogonality) and a weak ferromagnetic coupling is observed.[28,29,63,64] The values of the magnetic couplings for compounds **3**, **6**, and **9** lie within the range reported for previous examples exhibiting this last parallel arrangement of magnetic orbitals (J ranging from $+3$ to -45 cm^{-1}).

Acknowledgment. This work was supported by the Universidad del País Vasco/Euskal Herriko Unibertsitatea (UPV/EHU) (Project 169.310-EA857/2000), the Spanish Dirección General de Investigación Científica y Técnica (DGICYT) (Project 97-1397), and a predoctoral fellowship (AP 99/18598566).

Supporting Information Available: X-ray crystallographic files in CIF format. This material is available free of charge via the Internet at http://pubs.acs.org.

IC0103401

(61) (a) Hall, J. W. Ph.D. Dissertation, University of North Carolina, 1977. (b) Bonner, J.; Fisher, M. E. *Phys. Rev.* **1964**, *135*, A640.
(62) Kahn, O. *Comments Inorg. Chem.* **1984**, *3*, 105.
(63) Smekal, Z.; Travnicek, Z.; Lloret, F.; Marek, J. *Polyhedron* **1999**, *18*, 2787.
(64) Calatayud, M. L.; Castro, I.; Sletten, J.; Lloret, F.; Julve, M. *Inorg. Chim. Acta* **2000**, *300*, 846.